Transferable total-energy parametrizations for metals: Applications to elastic-constant determination

M. M. Sigalas* and D. A. Papaconstantopoulos
Complex Systems Theory Branch, Naval Research Laboratory, Washington, D.C. 20375-5320
(Received 16 March 1993)

In this work we present a method of fitting augmented-plane-wave energy bands and total-energy results for the fcc and bcc structures to a nonorthogonal tight-binding Hamiltonian from which the sum of the eigenvalues is derived, and to a simple pair potential that is designed to account for all the other terms of the total-energy expression. We have applied this method to calculate the elastic constants of the metals Rh, Pd, Ta, Ir, and Au, avoiding the expensive first-principles calculations of the distorted structures. We obtained very good agreement with both first-principles local-density-functional-theory calculations and experiment.

I. INTRODUCTION

A detailed understanding of the energies in nonperiodic structures (such as point or extended defects) in metals and alloys is very important in many problems in solid-state physics and materials science. The study of these defects, since they correspond to low-symmetry structures, requires techniques that can handle a large number of atoms per unit cell. For that reason it is often impractical to use *ab initio* calculations. Many models have been proposed in order to overcome this problem. In these models the total energy $E_{\rm tot}$ consists of a band-structure term describing the eigenvalue sum $E_{\rm bs}$, and a pair-potential term $E_{\rm pp}$:[1-4]

$$E_{\rm tot}=E_{\rm bs}+E_{\rm pp}\ . \tag{1}$$

Such expressions can be used to fit the results of first-principles total-energy calculations at given high-symmetry structures, and then use them to obtain the total energy of another configuration of atoms. The justification of this approach is given by Foulkes and Haydock[5] using density-functional theory.

The most commonly used model for metals is the embedded-atom method[1] (EAM) which has been successful in dealing with bulk and surface phonons, vacancies, impurities, etc.[1] This method is computationally fast but it requires certain experimental quantities as input. Also, the EAM does not give a reasonable estimate of the band structure for different configurations. Recently, a many-body alloy Hamiltonian (MBAH) method has been proposed and applied to investigate the effect of absorbates on surface vibrations by calculating the phonon spectra of clean and hydrogen-covered (001) and (110) surfaces of Pd.[2] Further testing of these methods to other systems is important in order to evaluate their usefulness.

Various tight-binding (TB) models have been used for semiconductors, in particular for Si and C.[6,7] They have been successful in the study of bulk and surface phonons, liquid phases, defects, surface reconstructions, etc., and more recently the structure and energetics of the newly discovered fullerenes.[8] As stated by several authors[3,5] the TB method has firm *ab initio* foundations and although it is computationally more demanding compared with pairwise potentials, it is orders of magnitude faster than the classic local-density techniques such as linear augmented plane wave and linear muffin-tin orbital. Application of the TB method to metals with an accuracy comparable to the first-principles methods is an open question.

In this paper we have tested the MBAH against our own implementation of the TB method in several metals. We fitted the total-energy expression Eq. (1) to augmented plane-wave (APW) total-energy results for the fcc and bcc structures; and then used Eq. (1) as an interpolation formula to calculate the total energy of the hcp structure and the elastic constants for the following metals: Rh, Pd, Ta, Ir, and Au.

II. THE MANY-BODY ALLOY HAMILTONIAN METHOD

Zhong, Li, and Tomanek constructed what they called a many-body alloy Hamiltonian as follows. In the second-moment approximation, $E_{\rm bs}$ in Eq. (1) is proportional to the effective bandwidth which in turn is proportional to the square root of the second moment M_2 of the local density of states, so[2]

$$E_{\rm bs}\propto M_2^{1/2}=\left[\sum_{j\neq i}t_{ij}^2\right]^{1/2}, \tag{2}$$

where t_{ij} is the hopping integral between neighboring sites i and j. Assuming an exponential distance dependence for the hopping integrals as well as for the pair-potential term in Eq. (1), they obtained[2]

$$E_{\rm tot}=-\left\{\sum_{j\neq i}\xi_0^2\exp\left[-2d\left[\frac{r_{ij}}{r_0}-1\right]\right]\right\}^{1/2}+\epsilon_0\sum_{j\neq i}\exp\left[-p\left[\frac{r_{ij}}{r_0}-1\right]\right], \tag{3}$$

where r_{ij} is the distance between atom i and j and the sums are over the neighbors. There are five parameters (ξ_0, d, ϵ_0, p, r_0) in this method which could be determined

by fitting results from *ab initio* calculations for high-symmetry structures.

Zhong, Li, and Tomanek,[2] applied this method to the Pd-H system. They determined the corresponding parameters by fitting local-density approximation (LDA) results for Pd and H in the fcc structures and PdH in the NaCl structure; they used this method to calculate the phonon spectra of clean and hydrogen-covered surfaces of Pd. Their surface results are in good agreement with experimental and LDA results although there are some significant differences, with the most notable one being that their calculated surface energy for Pd(110) is 0.73 eV/atom, while the corresponding LDA energy is 1.80 eV/atom.

We used the MBAH method to calculate elastic constants and vacancy formation energies of bulk Rh, Pd, Ir, and Au. We determined the parameters of the MBAH for each element by fitting our APW total-energy results for the fcc and bcc structures[9] to the total-energy expression Eq. (3).

We found that the results depend on the number of neighbors in Eq. (3); so it was necessary to use up to the third-nearest neighbor for Pd, Rh, and Au, and up to the second-nearest neighbor for Ir. The five parameters for each element are given in Table I. The difference between the MBAH method and APW results after the fitting procedure was less than 1 mRy so the bulk modulus and the equilibrium volume for both fcc and bcc structures, as well as the fcc-bcc structural total-energy difference, are nearly the same.

In order to calculate the elastic constants $C_{11}-C_{12}$ and C_{44}, an orthorhombic and a monoclinic strain[10] was applied to the MBAH; we calculate the elastic constants[10] from the difference in total energies of the distorted and undistorted lattices. The results are given in Table II and compared with the corresponding experimental results; the differences are less than 30% for both Pd and Ir but there are greater differences for Rh and Au. The most significant difference is for $C_{11}-C_{12}$ of Rh (Table II). Also, we calculated the vacancy formation energies E_v of these metals (Table II). In this calculation we do not take into account relaxation, but we expect this to be a small error,[11] which cannot explain the large discrepancy from experiment in Au.

In addition, we also tried without success to apply this method to metals that lie in the middle or in the beginning of the d rows; either the fitting errors were large or the predicted values were in poor agreement with experimental or LDA results. This is probably related to the second-moment approximation made in deriving Eq. (2), which is expected to work well only for elements with nearly filled d shells.[12]

TABLE I. Parameters for many-body alloy method as calculated by fitting the APW total-energy results to Eq. (2).

Element	ξ_0 (Ry)	ϵ_0 (mRy)	d	p	r_0 (a.u.)
Rh	0.280 97	6.6951	2.302 01	9.220 08	6.075 48
Pd	0.107 16	3.4279	2.627 17	12.751 86	5.541 38
Ir	0.189 05	1.4818	1.670 54	18.041 03	5.676 66
Au	0.121 95	3.4375	3.158 84	10.177 80	6.611 59

TABLE II. Elastic constants and vacancy formation energies (E_v) as calculated from the many-body alloy method. (Experimental results in parentheses.)

Element	C_{44} (Mbar)	$C_{11}-C_{12}$ (Mbar)	E_v (Ry)
Rh	1.70	0.94	0.378
	(1.84)	(2.19)	
Pd	1.07	0.75	0.139
	(0.71)	(0.58)	(0.103)
Ir	2.91	2.46	0.350
	(2.62)	(3.41)	
Au	0.76	0.45	0.141
	(0.42)	(0.29)	(0.066)

III. TIGHT-BINDING METHOD

In our implementation of the TB method we do not make the second-moment approximation; instead we rewrite Eq. (1) as follows:

$$E_{\text{tot}}=\sum_k \epsilon_k+\frac{1}{2}\sum_{j\neq i}\left\{\sum_n \frac{A_n}{r_{ij}^n}\right\}e^{\lambda r_{ij}}+c\ . \tag{4}$$

The first term is the sum of the eigenvalues of the occupied states of a one-electron Hamiltonian and the second is a repulsive pair potential that is a function of the bond length r_{ij}. In the second term, the outer sum is over the bond length r_{ij} and the inner sum represents a polynomial in r_{ij}^{-1}. *The constant c accounts for the scale difference between TB and APW results and of course cancels out when we take total-energy differences.* The sum of the eigenvalues is determined by a TB Hamiltonian that is fit, in the manner of Slater and Koster[13] to the individual eigenvalues of first-principles APW calculations.[9] This TB Hamiltonian involves s, p, and d orbitals, includes first-nearest-neighbor interactions, and is *nonorthogonal.* So for a transition element, the Hamiltonian is a 9×9 matrix that contains 20 hopping integrals and 4 on-site energies (see Table III to clarify the notation). The hopping integrals are determined by fitting the APW energy bands of the fcc structure for six different lattice parameters, which correspond to an interval approximately $\pm10\%$ from the equilibrium lattice constant. On the other hand, the on-site parameters are fitted only at the equilibrium lattice constant and kept fixed for the others. For a typical transition metal and for each lattice constant we fit six valence bands at 33 k-points in the $\frac{1}{48}$ of the Brillouin zone. The fit has an rms error of approximately 5 mRy for all six bands. In the next step we fit each TB parameter individually to a second-order polynomial with respect to the bond length r_{ij}; the fitting is nearly perfect. We expect that for lattice constants much different from the equilibrium this simple fitting function may not be sufficient, but in the present case where it is close to equilibrium volume, it is quite good. Hence, we can compute the sum of eigenvalues in Eq. (4) at any distance r_{ij}. Then we determine the coefficients A_n and λ of the polynomial that represents the pair potential in Eq. (4). This is done by fitting to our first-principles values of the total energy

for the fcc and bcc structures.[9] Therefore, Eq. (1) becomes an accurate interpolation formula of the total energy as a function of the r_{ij}. This formula gives the volume dependence of the fcc and bcc structures to within about 1 mRy of accuracy over a range $\pm 15\%$ the equilibrium volume.

The above procedure ensures that the band structure is accurately reproduced by the present TB model, at least for the fcc structure and for volumes close to the equilibrium. In contrast, the resulting bcc band structure is not as accurate and the predicted eigenvalues differ from the APW eigenvalues by 50 mRy on the average. Since integrated quantities tend to converge more rapidly, the sum of the eigenvalues is obtained with much better accuracy.

In Fig. 1, we plot the $ss\sigma$ and $sd\sigma$ hopping integrals of Pd and Au relative to the lattice constant as calculated from the present model and compared with the Harrison scaling (HS) law[14] (denoted by H in Fig. 1). The $ss\sigma$ parameters are reasonably well described by the d^2 dependence of the HS law, especially for Au, but the $sd\sigma$ as well as the other parameters are very different from $d^{-7/2}$ dependence of the HS law. The scaling of the TB parameters plays an important role in the model. Using the HS law in the fitting procedure instead of following the procedure described above, we found large errors in the predicted elastic constants and the total energy of the hcp structure. Also, since we find no universal scaling law similar to the HS law, we have to make fits for each element. The fitting parameters for the hopping integrals are presented in Table III. We note that we have fixed the on-site parameters to their values at the equilibrium lattice constant. This introduced an error in the energy bands at other lattice parameters, but it improved the fitting to the total energies.

The parameters for the repulsive potential [second term in Eq. (4)] found from the total-energy fitting are given in Table IV. We used 7 parameters for Ta, Pd, Ir, Rh, and 11 parameters for Au.

In Fig. 2 we show, as an example, the total energy as a function of volume for Rh and Ta in the fcc, bcc, and hcp structures as computed by Eq. (4). With our method we fit the fcc total energies almost exactly for all the elements; the bcc total energies are fitted less accurately (the Ta is the only exception) as shown by the broken lines in Fig. 2. We do not fit the total energies of the hcp structure; we compute it directly from Eq. (4) for the ideal c/a ratio. This neglects the fact that due to the reduced symmetry of the hcp lattice there are three d-like on-site parameters instead of two in the cubic structure. However, it should be stressed that this is a very good approximation because as shown in Table III the t_{2g} and ϵ_g parameters are nearly equal and also the three d-on-sites in the hcp are also found to be nearly equal (see Ref. 13). *We also set the dp-on-site parameter for the hcp structure equal to zero. Note that this parameter is usually an order of magnitude smaller than the other on-site parameters.* The differences between predictions from the TB model results and the APW results are very small for the fcc and bcc structures that we fit. For the hcp structure our

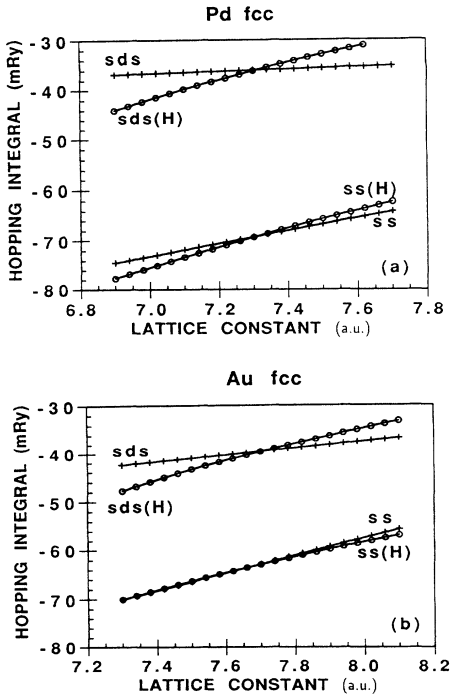

FIG. 1. Distance dependence of the $ss\sigma$ and $sd\sigma$ tight-binding parameters for (a) Pd and (b) Au. Comparison with the Harrison scaling law is shown.

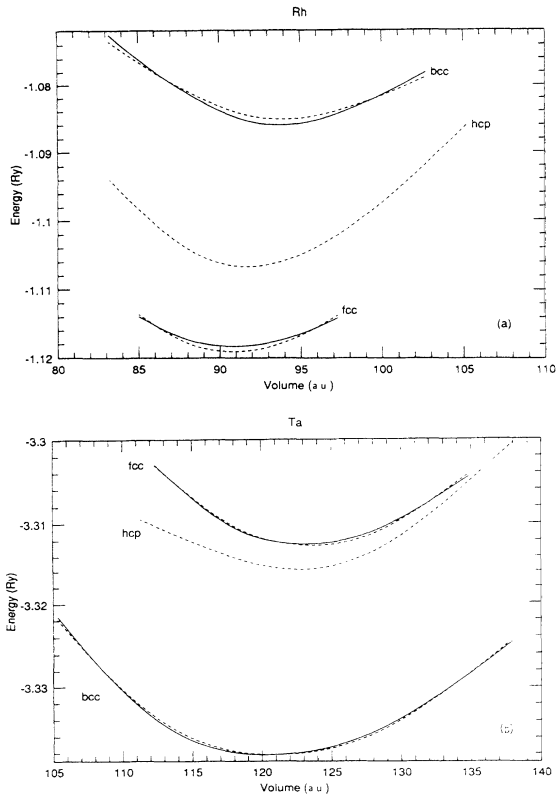

FIG. 2. Total energy of (a) Rh and (b) Ta as a function of volume. Solid lines show the APW results; broken lines show the results of the fit.

TABLE III. Coefficients in $F(r)=A+Br+Cr^2$ that fit the tight-binding parameters for Rh, Pd, Ta, Ir, and Au.

	Rh		Pd		Ta		Ir			Au	
	A (Ry)	B (Ry)	A (Ry)	B (Ry)	A (Ry)	B (Ry)	A (Ry)	B (Ry)	C (Ry)	A (Ry)	B (Ry)
						On site					
s	0.985 505	0.000 000	0.958 527	0.000 000	0.716 805	0.000 000	1.141 852	0.000 000	0.000 000	0.687 708	0.000 000
p	1.750 892	0.000 000	1.781 764	0.000 000	1.349 181	0.000 000	2.832 872	0.000 000	0.000 000	1.320 388	0.000 000
t_{2g}	0.537 927	0.000 000	0.401 713	0.000 000	0.809 257	0.000 000	0.554 607	0.000 000	0.000 000	0.238 407	0.000 000
ϵ_g	0.533 228	0.000 000	0.396 944	0.000 000	0.795 312	0.000 000	0.532 321	0.000 000	0.000 000	0.231 731	0.000 000
						Energy integrals					
$ss\sigma$	−0.205 447	0.026 038	−0.162 665	0.018 079	−0.052 108	0.000 606	−0.100 210	0.006 596	0.000 000	−0.201 828	0.025 524
$pp\sigma$	−0.173 395	0.032 273	−0.289 584	0.054 067	−0.612 521	0.095 010	−7.374 773	2.650 703	−0.234 912	−0.324 386	0.059 401
$pp\pi$	−0.344 984	0.049 453	−0.406 994	0.060 464	−0.441 900	0.060 201	−3.548 497	1.227 856	−0.108 312	−0.373 361	0.054 344
$dd\sigma$	−0.158 908	0.023 485	−0.168 219	0.024 834	−0.079 929	0.008 499	−0.169 718	0.024 160	0.000 000	−0.178 874	0.025 480
$dd\pi$	0.161 928	−0.025 963	0.198 046	−0.031 587	0.240 683	−0.032 219	0.284 824	−0.045 255	0.000 000	0.208 812	−0.032 990
$dd\delta$	−0.057 815	0.009 651	−0.080 165	0.013 265	−0.123 406	0.016 946	−0.109 266	0.017 585	0.000 000	−0.078 509	0.012 922
$sp\sigma$	0.030 383	0.005 199	−0.095 309	0.027 925	−0.283 898	0.051 013	−2.970 024	1.099 597	−0.099 823	−0.017 702	0.014 449
$sd\sigma$	−0.114 742	0.014 620	−0.050 518	0.002 812	0.095 636	−0.018 987	0.026 339	−0.011 112	0.000 000	−0.095 091	0.010 206
$pd\sigma$	−0.072 851	0.006 075	0.037 744	−0.014 190	0.369 053	−0.061 365	0.398 384	−0.080 284	0.000 000	−0.009 627	−0.006 062
$pd\pi$	0.234 964	−0.036 615	0.294 067	−0.046 555	0.314 369	−0.042 407	0.326 285	−0.051 340	0.000 000	0.254 744	−0.039 268
						Overlap integrals					
$ss\sigma$	0.138 029	−0.023 158	0.191 904	−0.031 784	0.119 375	−0.010 199	0.194 544	−0.028 193	0.000 000	0.182 962	−0.028 264
$pp\sigma$	−0.111 311	−0.009 843	−0.123 700	−0.006 017	−0.079 282	−0.018 435	−0.846 506	0.147 971	0.000 000	−0.177 303	0.002 156
$pp\pi$	−0.064 423	0.009 361	−0.084 035	0.012 608	−0.110 758	0.014 995	−0.119 365	0.016 209	0.000 000	−0.068 996	0.010 155
$dd\sigma$	0.137 212	−0.021 881	0.139 818	−0.020 784	0.191 879	−0.020 413	0.173 841	−0.021 394	0.000 000	0.180 623	−0.026 525
$dd\pi$	−0.003 787	0.003 758	−0.014 069	0.005 586	−0.064 464	0.011 988	−0.062 906	0.013 661	0.000 000	−0.023 952	0.006 597
$dd\delta$	−0.037 681	0.004 642	−0.038 163	0.004 282	−0.015 493	−0.001 194	−0.000 287	−0.003 404	0.000 000	−0.034 614	0.003 811
$sp\sigma$	−0.144 326	0.011 480	−0.155 105	0.013 212	−0.166 575	0.010 279	−0.456 421	0.074 390	0.000 000	−0.175 635	0.016 627
$sd\sigma$	0.265 218	−0.047 382	0.279 076	−0.047 299	0.193 842	−0.019 362	0.235 645	−0.032 604	0.000 000	0.246 189	−0.038 472
$pd\sigma$	0.144 538	−0.015 438	0.450 319	−0.073 010	0.288 778	−0.024 916	0.570 486	−0.090 141	0.000 000	0.358 951	−0.053 373
$pd\pi$	−0.055 130	0.019 093	0.110 012	−0.013 574	0.045 041	−0.002 548	−0.045 710	0.014 816	0.000 000	0.017 063	0.001 789

TABLE IV. Parameters of the pair-potential term [see Eq. (4)] for Rh, Pd, Ta, Ir, and Au.

	Rh	Pd	Ta	Ir	Au
λ	0.142 391	0.147 557	0.539 694	1.133 884	−0.812 931
c	−5.909 603	−8.414 009	−6.850 986	−10.411 475	−7.456 517
A_5	4.708 105*e*2	4.544 147*e*2	1.680 281*e*2	45.006 945	3.446 769*e*5
A_4	−32.900 886	−47.365 641	−19.633 534	−12.187 383	−3.350 766*e*4
A_3	−13.131 132	−13.423 783	−2.070 528	−2.056 867	−1.070 698*e*4
A_2	−1.105 297	−0.683 489	−0.530 902	0.881 607	−1.140 988*e*3
A_1	0.483 387	0.473 423	0.144 904	−0.067 953	54.262 295
A_0					46.345 168
A_{-1}					8.826 422
A_{-2}					0.055 621
A_{-3}					−0.182 364

results are less accurate, *as can be seen from the last column of Table V, which compares APW and TB results for hcp.* Our model includes only first-nearest neighbors and it has a repulsive potential without angular dependence [see Eq. (4)], so the repulsive potential for both fcc and hcp in ideal c/a ratio is exactly the same and the difference in the total energy comes only from the band-structure term. We can overcome this problem by including further neighbors. We have not addressed this problem yet because we concentrate on determining the elastic constants which, as shown below, are computed accurately by the present model.

An orthorhombic strain applied to our TB Hamiltonian yields total energies from Eq. (4) that were used to determine the elastic constant difference $C_{11}-C_{12}$ from the expression

$$\Delta E(x)=(C_{11}-C_{12})V_0x^2 \tag{5}$$

and the elastic constant C_{44} from

$$\Delta E(x)=C_{44}\frac{V_0}{2}x^2 , \tag{6}$$

where $\Delta E(x)$ is the energy change corresponding to a distortion x (Ref. 11) and V_0 is the equilibrium volume. Our results for C_{ij} are shown in Table V, where they are compared with measured values[15] and first-principles calculations.[16] The differences from the experiment are less than 15% for Ta, Ir, and Rh, and less than 30% for Pd and Au (note that they both have small elastic constants). The corresponding results using the MBAH method (Table II) have larger discrepancies from experiment. Taking into account that even the most accurate first-principles LAPW calculations[15] have a difference of about 10% from experiment, and the systematically correct prediction of the elastic constants from the present model, we conclude that our TB model could be used for further, more complicated applications such as phonon spectra, surface calculations, molecular-dynamics simulations, etc., with results comparable to first-principles calculations.

In order to check the importance of the bcc structure in the fitting procedure we did an independent fitting to only the fcc total energies of Ir. The calculated elastic constants from this fitting were $C_{11}-C_{12}=2.66$ Mbar and $C_{44}=2.12$ Mbar, which are not as close to the experimental values as those from the fitting of both fcc and bcc total energies shown in Table V. Also, preliminary results show that by the inclusion of second-nearest neighbors in our model, we get smaller errors in the fitting procedure and improve the predicted results.

IV. CONCLUSIONS

We have investigated total-energy expressions that consist of a term describing the eigenvalue sum and a pair-potential term. Such expressions can be used to fit the results of first-principles total-energy calculations at given structures, and then obtain the total energy of another configuration of atoms avoiding the complexity of further *ab initio* calculations. We have checked the MBAH method[2] and the TB Hamiltonian method.

Using the MBAH method we can predict in relatively good agreement with experiment the elastic constants and the vacancy formation energies of some of the ele-

TABLE V. Elastic constants C_{ij}, bulk modulus B, and the equilibrium energies of bcc (E_b) and hcp (E_h) structures relative to the fcc as calculated from the TB model (first line). The values in the second (third) line are the experimental (Ref. 15) [first-principles (Refs. 9 and 16)] values where available.

Element	C_{44} (Mbar)	C_{11} (Mbar)	C_{12} (Mbar)	B (Mbar)	E_b (mRy)	E_h (mRy)
Rh	2.09	5.554	3.044	3.881	34.1	13.6
	1.84	4.165	1.975	2.705		
				3.116	33.0	6.6
Pd	0.85	2.984	2.214	2.471	12.0	14.6
	0.71	2.340	1.760	1.808		
	0.65	2.383	1.793	1.990	9.6	5.0
Ta	0.83	2.612	1.702	2.005	−25.5	−3.0
	0.82	2.650	1.590	2.001		
				2.008	−25.7	53.6
Ir	2.47	6.312	3.132	4.192	52.5	32.9
	2.62	5.823	2.413	3.550		
	2.60	6.210	2.560	3.763	50.8	11.9
Au	0.37	2.048	1.688	1.808	6.1	2.0
	0.42	2.020	1.700	1.732		
				1.689	8.6	1.6

ments at the end of the *d* rows, but this model completely fails for all elements at the beginning of the series.

In contrast, our implementation of the TB model can predict the elastic constants of *all* the metals that we considered in very good agreement with both experiment and *ab initio* total-energy calculations. This method eliminates the need to do the very expensive first-principles calculations that include the orthorhombic and monoclinic distortions of the lattice that are used to calculate elastic constants. The applications of this model in calculating phonon spectra, surface properties, and performing molecular-dynamics simulations seems very promising.

ACKNOWLEDGMENTS

We wish to acknowledge discussions with J. Q. Broughton, R. E. Cohen, B. M. Klein, M. J. Mehl, W. E. Pickett, D. J. Singh, and A. J. Skinner. This work was supported in part by the U.S. Office of Naval Research.

---

*Present address: Ames Laboratory, Physics Department, Iowa State University, Ames, IA 50011-3020.

[1]S. M. Foiles, M. I. Baskes, and M. S. Daw, Phys. Rev. B **33**, 7983 (1986); M. S. Daw, *ibid.* **39**, 7441 (1989).

[2]W. Zhong, Y. S. Li, and D. Tomanek, Phys. Rev. B **44**, 13 053 (1991).

[3]M. W. Finnis, A. T. Paxton, D. G. Pettifor, A. P. Sutton, and Y. Ohta, Philos. Mag. A **58**, 143 (1988).

[4]A. P. Sutton, M. W. Finnis, D. G. Pettifor, and Y. Ohta, J. Phys. C **21**, 35 (1988).

[5]W. M. C. Foulkes and R. Haydock, Phys. Rev. B **39**, 12 520 (1989).

[6]C. H. Xu, C. Z. Wang, C. T. Chan, and K. M. Ho, J. Phys. Condens. Matter **4**, 6047 (1992).

[7]L. Goodwin, A. J. Skinner, and D. G. Pettifor, Europhys. Lett. **9**, 701 (1989).

[8]B. L. Zhang, C. H. Xu, C. Z. Wang, C. T. Chan, and K. M. Ho, Phys. Rev. B **46**, 7333 (1992).

[9]M. Sigalas, D. A. Papaconstantopoulos, and N. C. Bacalis, Phys. Rev. B **45**, 5777 (1992).

[10]M. J. Mehl, J. E. Osburn, D. A. Papaconstantopoulos, and B. M. Klein, Phys. Rev. B **41**, 10 311 (1990).

[11]M. S. Daw and M. I. Baskes, Phys. Rev. B **29**, 6443 (1984).

[12]D. Tomanek, S. Mukherjee, and K. H. Bennemann, Phys. Rev. B **28**, 665 (1983); D. Tomanek, A. A. Aligia, and C. A. Balseiro, *ibid.* **32**, 5051 (1985).

[13]J. C. Slater and G. F. Koster, Phys. Rev. **94**, 1498 (1954); D. A. Papaconstantopoulos, *Handbook of the Band Structure of Elemental Solids* (Plenum, New York, 1986).

[14]W. A. Harrison, *Electronic Structure and the Properties of Solids* (Freeman, San Francisco, 1980).

[15]G. Simmons and H. Wang, *Single Crystal Elastic Constants and Calculated Aggregate Properties: A Handbook,* 2nd ed. (MIT, Cambridge, MA, 1971); N. W. Ashcroft and N. D. Mermin, *Solid State Physics* (Saunders, Philadelphia, 1976); D. K. Hsu and R. G. Leisure, Phys. Rev. B **20**, 1339 (1979).

[16]M. J. Mehl, B. M. Klein, and D. A. Papaconstantopoulos, in *Intermetallic Compounds—Principles and Practice,* edited by J. H. Westbrook and R. L. Fleischer (Wiley, London, 1993), Vol. 1, Chap. 9.